

# Disentangling the role of the $Y(4260)$ in $e^+e^- \rightarrow D^*\bar{D}^*$ and $D_s^*\bar{D}_s^*$ via line shape studies

Si-Run Xue<sup>1,3,a</sup>, Hao-Jie Jing<sup>2,3,b</sup>, Feng-Kun Guo<sup>2,3,c</sup>, and Qiang Zhao<sup>1,3,4,d</sup>

<sup>1</sup>*Institute of High Energy Physics and Theoretical Physics Center for Science Facilities,  
Chinese Academy of Sciences, Beijing 100049, China*

<sup>2</sup>*CAS Key Laboratory of Theoretical Physics, Institute of Theoretical Physics,  
Chinese Academy of Sciences, Beijing 100190, China*

<sup>3</sup>*School of Physical Sciences, University of Chinese Academy of Sciences, Beijing 100049, China and*

<sup>4</sup>*Synergetic Innovation Center for Quantum Effects and Applications (SICQEA),  
Hunan Normal University, Changsha 410081, China*

(Dated: September 10, 2018)

Whether the  $Y(4260)$  can couple to open charm channels has been a crucial issue for understanding its nature. The available experimental data suggest that the cross section line shapes of exclusive processes in  $e^+e^-$  annihilations have nontrivial structures around the mass region of the  $Y(4260)$ . As part of a series of studies of the  $Y(4260)$  as mainly a  $\bar{D}D_1(2420) + c.c.$  molecular state, we show that the partial widths of the  $Y(4260)$  to the two-body open charm channels of  $e^+e^- \rightarrow D^*\bar{D}^*$  and  $D_s^*\bar{D}_s^*$  are much smaller than that to  $\bar{D}D^*\pi + c.c.$ . The line shapes measured by the Belle Collaboration for these two channels can be well described by the vector charmonium states  $\psi(4040)$ ,  $\psi(4160)$  and  $\psi(4415)$  together with the  $Y(4260)$ . It turns out that the interference of the  $Y(4260)$  with the other charmonia produces a dip around 4.22 GeV in the  $e^+e^- \rightarrow D^*\bar{D}^*$  cross section line shape. The data also show an evidence for the strong coupling of the  $Y(4260)$  to the  $D\bar{D}_1(2420)$ , in line with the expectation in the hadronic molecular scenario for the  $Y(4260)$ .

PACS numbers: 14.40.Rt, 14.40.Pq

---

<sup>a</sup> *E-mail address:* xuesr@ihep.ac.cn

<sup>b</sup> *E-mail address:* jinghaojie@itp.ac.cn

<sup>c</sup> *E-mail address:* fkguo@itp.ac.cn

<sup>d</sup> *E-mail address:* zhaoq@ihep.ac.cn

## I. INTRODUCTION

The mysterious state  $Y(4260)$  has attracted a lot of attention since its observation in 2005 by the BaBar Collaboration [1]. Although many different models were proposed as solutions in the literature, it is unfortunate that not all of these scenarios have been systematically studied and compared with the existing experimental data (see e.g. several recent reviews [2–5] for summaries of some theoretical interpretations proposed in the literature). Following a series of recent studies by treating the  $Y(4260)$  as mainly a  $\bar{D}D_1(2420) + c.c.$  hadronic molecule, we are motivated to examine as many as possible exclusive processes where the  $Y(4260)$  can contribute. Such systematic studies with more experimental constraints would either support or invalidate the picture of the  $Y(4260)$  being a hadronic molecule of  $\bar{D}D_1(2420) + c.c.$  and should provide more insights into its intrinsic structure. Therefore, we investigate the cross section line shapes of the  $e^+e^- \rightarrow D^*\bar{D}^*$  and  $D_s^*\bar{D}_s^*$  processes which cover the mass region of the  $Y(4260)$  and contain several established conventional charmonium states, i.e.,  $\psi(4040)$ ,  $\psi(4160)$  and  $\psi(4415)$ .

So far, it has been demonstrated that most of the puzzling observations in the mass region of  $Y(4260)$  in  $e^+e^-$  annihilations can be accounted for in the same framework self-consistently. For the strong  $S$ -wave interactions between  $\bar{D}$  and  $D_1(2420)$  (the charge conjugation,  $D\bar{D}_1(2420)$ , is always implicated in the calculations), the dynamically generated  $Y(4260)$  should contain a large molecular component of  $\bar{D}D_1(2420) + c.c.$  as the long-distance component of its wave function, while a small short-distance component is always allowed. The consequence is that the  $Y(4260)$  will dominantly decay into  $\bar{D}D^*\pi + c.c.$  via the decays of its constituent hadrons [6–8]. Moreover, due to the strong  $S$ -wave coupling to the nearby  $\bar{D}D_1(2420)$  channel, the cross section line shape for the  $e^+e^- \rightarrow \bar{D}D^*\pi + c.c.$  process should not be described by a Breit–Wigner parametrization. This is generally true for any states that strongly couple to nearby thresholds via an  $S$ -wave interaction. Namely, it is natural to expect a nontrivial cross section line shape for  $e^+e^- \rightarrow \bar{D}D^*\pi + c.c.$  around the mass of the  $Y(4260)$ . This phenomenon has been investigated in detail in Refs. [7, 8] which are closely correlated with the study of the nature of the charged charmonium states  $Z_c(3900)$ . The experimental data, i.e., the cross sections for  $e^+e^- \rightarrow J/\psi\pi\pi$ ,  $h_c\pi\pi$  and the invariant mass spectra as well as angular distributions of  $Y(4260) \rightarrow \bar{D}D^*\pi + c.c.$ , which were also motivated by the search for  $Z_c(3900)$  and  $Z_c(4020)$  at BESIII [9–14], have provided important constraints on the molecular component of the  $Y(4260)$ .

One interesting question arising from the above mentioned analysis is whether the  $Y(4260)$  should have significantly large decay widths into other open charm channels apart from  $\bar{D}D^*\pi + c.c.$ .

Given that the total width of  $Y(4260)$  is dominated by the  $\bar{D}D^*\pi + c.c.$  channel [15], which has a partial width of about 65 MeV in Ref. [8], while its decays into the hidden charm channels, i.e.  $J/\psi\pi\pi$ ,  $h_c\pi\pi$ , and  $\chi_{c0}\omega$ , turn out to be relatively small, the  $Y(4260)$  decays into other open charm channels should also have small widths in order to match the total width extracted in the combined analysis of  $e^+e^- \rightarrow J/\psi\pi\pi$ ,  $h_c\pi\pi$ , and  $\bar{D}D^*\pi + c.c.$  In this sense, to accommodate the experimental data for  $e^+e^- \rightarrow D^*\bar{D}^*$  and  $D_s^*\bar{D}_s^*$  in the same framework is a challenge for the molecular picture, and should provide more information about its structure.

In this work, we analyze the cross section line shapes of the  $e^+e^- \rightarrow D^*\bar{D}^*$  and  $D_s^*\bar{D}_s^*$  processes from threshold to about 4.6 GeV. These two processes have been measured by the Belle Collaboration using the initial state radiation (ISR) in  $e^+e^-$  annihilations [16, 17]. One can see that the cross sections for  $e^+e^- \rightarrow D^*\bar{D}^*$  have been measured with a high precision [16], but there are still large uncertainties in the data for  $e^+e^- \rightarrow D_s^*\bar{D}_s^*$  [17]. The former process has been studied in [18] which considers the  $P$ -wave coupled-channel effects due to a pair of ground state charmed mesons and the  $\psi(4040)$  but not the  $Y(4260)$ . In our analysis, in addition to the  $Y(4260)$  which is included as a  $\bar{D}D_1(2420)$  hadronic molecule, we also include several conventional vector charmonium states established in this mass region including the  $\psi(4040)$ , the  $\psi(4160)$  and the  $\psi(4415)$ . We try to understand the behavior of the molecular state  $Y(4260)$  in this energy region and its interference with other charmonium states in the description of the cross section line shapes. We note in advance that our focus is mainly in the vicinity of the  $Y(4260)$ , i.e. around the threshold of  $\bar{D}D_1(2420)$ . Although there are additional exotic candidates above the  $\bar{D}D_1(2420)$  threshold, such as the  $Y(4360)$ , to be neglected in this analysis, we find that we can still draw a clear conclusion on the  $Y(4260)$  contribution due to the relatively isolated  $\bar{D}D_1(2420)$  threshold.

In this paper, we first estimate the partial decay width of  $Y(4260) \rightarrow D^*\bar{D}^*$  in the molecular picture in Sec. II, and then we study the cross section line shapes of  $e^+e^- \rightarrow D^*\bar{D}^*$  and  $D_s^*\bar{D}_s^*$  considering the  $Y(4260)$  and three charmonium states mentioned above in Sec. III. A brief summary will be given in Sec. IV.

## II. THE PARTIAL DECAY WIDTH OF $Y(4260) \rightarrow D^*\bar{D}^*$

In our scenario, the  $Y(4260)$  is treated as mainly an  $S$ -wave molecule of  $\bar{D}D_1(2420) + c.c.$  with a small mixture of a compact  $c\bar{c}$  core [8]. This treatment recognizes the HQSS breaking in the production of  $Y(4260)$  via  $e^+e^-$  annihilations. Namely, its production in  $e^+e^-$  annihilations is mainly via the direct coupling to its compact  $c\bar{c}$  core which contains the  $^3S_1(c\bar{c})$  configuration.

Then, the HQSS breaking allows the mixture of the  ${}^3S_1(c\bar{c})$  core with the long-distance component of  $\bar{D}D_1(2420) + c.c.$  which can couple to  ${}^3D_1(c\bar{c})$  via an  $S$ -wave interaction. The wave function renormalization will dress the nonvanishing  $\gamma^* - {}^3S_1(c\bar{c})$  coupling and the coupling of  $Y(4260)$  to  $\bar{D}D_1(2420) + c.c.$  as investigated in Ref. [8]. As a result of this scenario, it allows for the decay of  $Y(4260) \rightarrow D^*\bar{D}^*$  to occur not only via the dominant  $\bar{D}D_1(2420) + c.c.$  component but also through the direct coupling of the  $c\bar{c}$  core to  $D^*\bar{D}^*$  as illustrated in Fig. 1.

In the framework of non-relativistic effective field theory (NREFT) the Lagrangians for the coupling vertices in Fig. 1 can be written as [7, 8, 19, 20]

$$\mathcal{L}_{YD_1\bar{D}} = i\frac{y^{\text{eff}}}{\sqrt{2}}(\bar{D}_a^\dagger Y^i D_{1a}^{i\dagger} - \bar{D}_{1a}^{i\dagger} Y^i D_a^\dagger) + H.c., \quad (1)$$

$$\mathcal{L}_{D_1D^*\pi} = i\frac{h'}{f_\pi} \left[ 3D_{1a}^i (\partial^i \partial^j \phi_{ab}) D_b^{*j\dagger} - D_{1a}^i (\partial^j \partial^j \phi_{ab}) D_b^{*i\dagger} + 3\bar{D}_{1a}^i (\partial^i \partial^j \phi_{ba}) \bar{D}_b^{*j\dagger} - \bar{D}_{1a}^i (\partial^j \partial^j \phi_{ba}) \bar{D}_b^{*i\dagger} \right] + H.c., \quad (2)$$

$$\mathcal{L}_{D^*D\pi} = g_\pi (D_a \partial^i \phi_{ab} D_b^{*i\dagger} + \bar{D}_a \partial^i \phi_{ba} \bar{D}_b^{*i\dagger}) + H.c., \quad (3)$$

where  $f_\pi = 132$  MeV and the effective coupling for  $Y(4260)$  and  $\bar{D}D_1(2420)$  is  $y^{\text{eff}} = (3.94 \pm 0.04)\text{GeV}^{-1/2}$  which has been determined by the combined analysis of  $e^+e^- \rightarrow J/\psi\pi\pi$ ,  $h_c\pi\pi$  and  $\bar{D}D^*\pi + c.c.$  [7, 8]; the effective coupling constants  $h'$  and  $g_\pi$  can be determined by the processes of  $D_1^0 \rightarrow D^{*+}\pi^-$  and  $D^{*-} \rightarrow D^0\pi^-$ , respectively. The direct coupling for  $Y(4260) \rightarrow D_{(s)}^*\bar{D}_{(s)}^*$  takes the same form as the vector charmonium couplings to  $D_{(s)}^*\bar{D}_{(s)}^*$  and will be given in the next section.

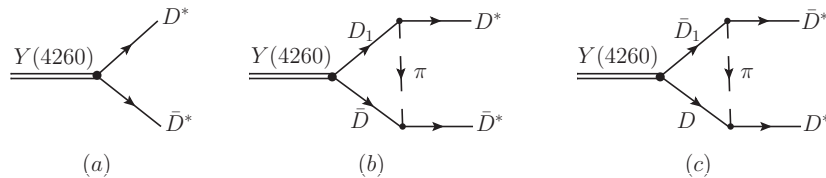


FIG. 1. Feynman diagrams for the two-body decay  $Y(4260) \rightarrow D^*\bar{D}^*$  in our scenario.

The decay amplitude for the loop diagrams in Fig. 1 (b) and (c) can then be expressed as

$$\begin{aligned}
\mathcal{M}_{Y(4260) \rightarrow D^* \bar{D}^*}^{\text{Loop}} &= \frac{3y^{\text{eff}} h' g_\pi}{2\sqrt{2} f_\pi} \epsilon_Y^i \epsilon_{D^*}^{j*} \epsilon_{\bar{D}^*}^{k*} \int \frac{d^4 l}{(2\pi)^4} \\
&\times \left\{ \frac{3l^i l^j l^k - \delta^{ij} l^k \vec{l}^2}{[(p_1 + l)^2 - m_{D_1}^2 + i0^+][(p_2 - l)^2 - m_D^2 + i0^+][l^2 - m_\pi^2 + i0^+]} \right. \\
&\quad \left. - \frac{3l^i l^j l^k - \delta^{ik} l^j \vec{l}^2}{[(p_2 + l)^2 - m_{D_1}^2 + i0^+][(p_1 - l)^2 - m_D^2 + i0^+][l^2 - m_\pi^2 + i0^+]} \right\} \\
&\equiv \frac{3y^{\text{eff}} h' g_\pi}{2\sqrt{2} f_\pi} \epsilon_Y^i \epsilon_{D^*}^{j*} \epsilon_{\bar{D}^*}^{k*} \left[ 3I^{ijk} - C^{ijk} - 3I^{ijk}(p_1 \leftrightarrow p_2) + C^{ikj}(p_1 \leftrightarrow p_2) \right] \\
&= \frac{3y^{\text{eff}} h' g_\pi}{2\sqrt{2} f_\pi} \epsilon_Y^i \epsilon_{D^*}^{j*} \epsilon_{\bar{D}^*}^{k*} \left( 6I^{ijk} - C^{ijk} - C^{ikj} \right), \tag{4}
\end{aligned}$$

where  $p_1$ ,  $p_2$  and  $l$  are the four momenta of the  $D^*$ ,  $\bar{D}^*$  and  $\pi$ , respectively. In the last step, we have used  $p_1^2 = p_2^2 = m_{D^*}^2$  and  $p_2^i = -p_1^i$  in the center-of-mass (c.m.) frame. The factor of 3/2 comes from the isospin symmetry and function  $C^{ijk}$  and  $I^{ijk}$  are defined as follows:

$$C^{ijk} \equiv \sum_{m=1}^3 \delta^{ij} I^{kmm}, \tag{5}$$

$$I^{ijk} \equiv \int \frac{d^4 l}{(2\pi)^4} \frac{l^i l^j l^k}{[(p_1 + l)^2 - m_{D_1}^2 + i0^+][(p_2 - l)^2 - m_D^2 + i0^+][l^2 - m_\pi^2 + i0^+]}. \tag{6}$$

It is interesting to compare the transition of Fig. 1 with the hidden charm decay channels such as  $Y(4260) \rightarrow Z_c(3900)\pi$  [8, 19] and  $\chi_{c0}\omega$  [21]. Following the NREFT power counting scheme of Refs. [5, 22, 23], it can be seen that the loop amplitude for the  $Y(4260) \rightarrow Z_c(3900)\pi$  is ultraviolet (UV) convergent and scales as  $1/v$  with  $v$  the typical non-relativistic velocity of the intermediate charmed mesons. With  $v \ll 1$  the loop integral gets enhanced in comparison with the tree diagram. The case for the  $Y(4260) \rightarrow \chi_{c0}\omega$  is similar. Such a power counting is because of the  $S$ -wave couplings of both the initial and final heavy particles to the intermediate charmed mesons.

For the  $Y(4260) \rightarrow D^* \bar{D}^*$ , the velocity scaling is different. Near the mass threshold of  $\bar{D}D_1(2420)$  the internal charmed mesons carry the typical velocity  $v \sim (|m_Y - m_D - m_{D_1}|/\tilde{m})^{1/2} \simeq 0.1$ , where  $\tilde{m} \equiv (m_D + m_{D_1})/2$ , and the velocity of the final  $D^*$  is  $v_f \simeq 0.35$  in the  $Y(4260)$  rest frame. For the velocity scaling, we may count  $v_f \sim v$ . Then the loop integral measure scales as  $v^5$ , and all propagators scale as  $v^{-2}$ . As a result, the triangle loop amplitude scales as  $v^5 v^{-6} v^3 = v^2$ , where the factor of  $v^3$  comes from the vertices, which is significantly suppressed in respect of the contact interaction. Because of the  $D$ - and  $P$ -wave pionic couplings given by Eqs. (2) and (3), respectively, the loop decay amplitude can be split into  $P$ -wave and  $F$ -wave parts as

$$I^{ijk} = \vec{p}_1^2 \left( p_1^i \delta^{jk} + p_1^j \delta^{ik} + p_1^k \delta^{ij} \right) I_P + \left[ p_1^i p_1^j p_1^k - \frac{1}{5} \vec{p}_1^2 \left( p_1^i \delta^{jk} + p_1^j \delta^{ik} + p_1^k \delta^{ij} \right) \right] I_F. \tag{7}$$

The first term contributes to the decay into the  $D^*\bar{D}^*$  in a  $P$ -wave, while the second contributes to that in a  $F$ -wave. While the  $F$ -wave part is UV convergent, the  $P$ -wave part diverges and needs to be regularized and renormalized. The UV divergence can be absorbed by introducing a counterterm. However, the tree-level term of Fig. 1 (a) cannot serve as the counterterm for the loop amplitude of Fig. 1 (b) and (c) since diagram (a) is introduced to incorporate the  ${}^3S_1(c\bar{c})$  coupling to  $D^*\bar{D}^*$  while in diagrams (b) and (c) the  $S$ -wave  $\bar{D}D_1(2420)$ , which leads to the transitions to  $D^*\bar{D}^*$ , couples to the  ${}^3D_1(c\bar{c})$  in the heavy quark limit [24]. This means that the UV divergence here needs to be absorbed into a different counterterm. Here we will regularize the UV divergence practically using a form factor with a cutoff, see below. The cutoff will be treated as a free parameter, which effectively takes the place of the counterterm at a given scale.

In order to regularize the UV contributions in the loop integral, we introduce a monopole form factor for each propagator to take into account the off-shell effects in the loop integral:

$$\mathcal{F}(\Lambda_i^2, m_i^2, l_i^2) = \frac{\Lambda_i^2 - m_i^2}{\Lambda_i^2 - l_i^2}, \quad (8)$$

where  $\Lambda_1 \equiv m_{D_1} + \alpha\Lambda_{\text{QCD}}$  and  $\Lambda_2 \equiv m_D + \alpha\Lambda_{\text{QCD}}$ , with  $\Lambda_{\text{QCD}} = 220$  MeV and  $\alpha$  a parameter of order unity, are defined for the heavy charmed mesons. For the light pion exchange the cut-off  $\Lambda_\pi$  is within a range of  $0.5 \sim 1$  GeV as usually adopted. Then the loop amplitude  $I^{ijk}$  can be expressed as:

$$\begin{aligned} I^{ijk} &= \int \frac{d^D l}{(2\pi)^D} \frac{l^i l^j l^k \mathcal{F}(\Lambda_1^2, m_{D_1}^2, (p_1 + l)^2) \mathcal{F}(\Lambda_2^2, m_D^2, (p_2 - l)^2) \mathcal{F}(\Lambda_\pi^2, m_\pi^2, l^2)}{[(p_1 + l)^2 - m_{D_1}^2 + i0^+][(p_2 - l)^2 - m_D^2 + i0^+][l^2 - m_\pi^2 + i0^+]} \\ &= \frac{i}{16\pi^2} [p_1^i p_1^j p_1^k A' + (-p_1^i \delta^{jk} - p_1^j \delta^{ik} - p_1^k \delta^{ij}) B'], \end{aligned} \quad (9)$$

with

$$\begin{aligned} A' &\equiv A(P^2, p_1^2, p_2^2, m_{D_1}^2, m_D^2, m_\pi^2) - A(P^2, p_1^2, p_2^2, \Lambda_1^2, m_D^2, m_\pi^2) - A(P^2, p_1^2, p_2^2, m_{D_1}^2, \Lambda_2^2, m_\pi^2) \\ &\quad - A(P^2, p_1^2, p_2^2, m_{D_1}^2, m_D^2, \Lambda_\pi^2) + A(P^2, p_1^2, p_2^2, \Lambda_1^2, \Lambda_2^2, m_\pi^2) + A(P^2, p_1^2, p_2^2, \Lambda_1^2, m_D^2, \Lambda_\pi^2) \\ &\quad + A(P^2, p_1^2, p_2^2, m_{D_1}^2, \Lambda_2^2, \Lambda_\pi^2) - A(P^2, p_1^2, p_2^2, \Lambda_1^2, \Lambda_2^2, \Lambda_\pi^2), \end{aligned} \quad (10)$$

$$\begin{aligned} B' &\equiv B(P^2, p_1^2, p_2^2, m_{D_1}^2, m_D^2, m_\pi^2) - B(P^2, p_1^2, p_2^2, \Lambda_1^2, m_D^2, m_\pi^2) - B(P^2, p_1^2, p_2^2, m_{D_1}^2, \Lambda_2^2, m_\pi^2) \\ &\quad - B(P^2, p_1^2, p_2^2, m_{D_1}^2, m_D^2, \Lambda_\pi^2) + B(P^2, p_1^2, p_2^2, \Lambda_1^2, \Lambda_2^2, m_\pi^2) + B(P^2, p_1^2, p_2^2, \Lambda_1^2, m_D^2, \Lambda_\pi^2) \\ &\quad + B(P^2, p_1^2, p_2^2, m_{D_1}^2, \Lambda_2^2, \Lambda_\pi^2) - B(P^2, p_1^2, p_2^2, \Lambda_1^2, \Lambda_2^2, \Lambda_\pi^2). \end{aligned} \quad (11)$$

Here the functions  $A$  and  $B$  are defined as

$$A(P^2, p_1^2, p_2^2, m_{D_1}^2, m_D^2, m_\pi^2) = \int_0^1 dx \int_0^1 \frac{y^4}{\Delta} dy, \quad (12)$$

$$B(P^2, p_1^2, p_2^2, m_{D_1}^2, m_D^2, m_\pi^2) = \int_0^1 dx \int_0^1 \frac{1}{2} y^2 \ln \Delta dy, \quad (13)$$

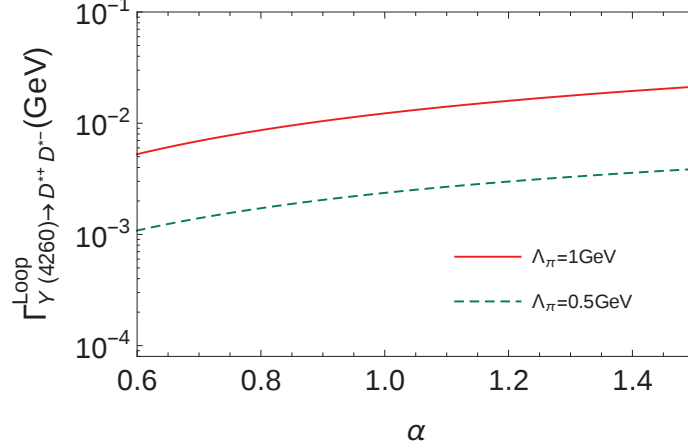


FIG. 2. The cutoff-dependence of the partial decay width of  $Y(4260) \rightarrow D^{*+}D^{*-}$  from the one-pion exchange diagrams in the molecular scenario. Here the results with two typical  $\Lambda_\pi$  values are shown.

where  $P \equiv p_1 + p_2$  is the initial momentum,  $x$  and  $y$  are the Feynman parameters, and  $\Delta = y^2 p_x^2 + (1-y)m_\pi^2 - y\Delta m_x^2$  with  $p_1 = xp_1 - (1-x)p_2$  and  $\Delta m_x^2 = x(p_1^2 - m_{D_1}^2) + (1-x)(p_2^2 - m_D^2)$ . In the numerical calculation, we replace  $m_{D_1}$  by  $m_{D_1} - i\Gamma_{D_1}/2$  with  $\Gamma_{D_1}$  the constant width of the  $D_1(2420)$ .

Due to the UV divergence in the  $P$ -wave part of the loop amplitude, it is impossible to make a definite prediction on the two-body decay partial width of the  $Y(4260)$  into a pair of vector charm mesons by simply calculating the loop diagrams. The best we can do is to estimate the values by varying the cutoffs in the form factors within natural ranges. Thus, in Fig. 2 we show the dependence of  $\Gamma_{Y(4260) \rightarrow D^{*+}D^{*-}}^{\text{Loop}}$  on  $\alpha$  with two typical values for  $\Lambda_\pi$ . The result ranges from 1 MeV to about 20 MeV in the figure, and for  $\alpha = 1$  it takes a value of 2.4 MeV and 12.3 MeV for  $\Lambda_\pi = 0.5$  GeV and 1 GeV, respectively. These values are significantly smaller than the partial width for  $Y(4260) \rightarrow \bar{D}D^*\pi + c.c.$

One intriguing feature of the  $Y(4260)$  is that it does not show up as a peak in the exclusive two-body open-charm cross sections. In order to clarify the role played by the  $Y(4260)$  in  $e^+e^- \rightarrow D^{*+}D^{*-}$ , we will investigate the cross section line shape of this process in the next section taking into account contributions from the nearby charmonium states. The idea is to investigate whether the cross section line shapes could provide more stringent constraint on  $Y(4260)$  or not. A combined investigation of the cross section line shape of  $e^+e^- \rightarrow D_s^{*+}D_s^{*-}$  will also be presented.

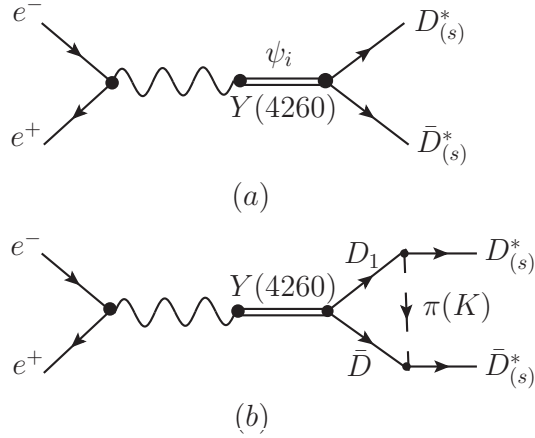


FIG. 3. Feynman diagrams for  $e^+e^- \rightarrow D_{(s)}^*\bar{D}_{(s)}^*$  via (a) intermediate charmonium states  $\psi_i$ , and (b)  $Y(4260)$  as a  $\bar{D}D_1(2420) + c.c.$  hadronic molecule state.

### III. THE LINE SHAPES OF THE CROSS SECTIONS OF $e^+e^- \rightarrow D_{(s)}^*\bar{D}_{(s)}^*$

In order to investigate the line shape of  $e^+e^- \rightarrow D_{(s)}^*\bar{D}_{(s)}^*$  in the vicinity of  $Y(4260)$ , the contributions from the nearby charmonium states,  $\psi(4040)$ ,  $\psi(4160)$  and  $\psi(4415)$ , which are normally considered as the  $3S$ ,  $2D$  and  $4S$  charmonium states, respectively, should be included. For convenience, we use  $\psi_1$ ,  $\psi_2$  and  $\psi_3$  to denote  $\psi(4040)$ ,  $\psi(4160)$  and  $\psi(4415)$ , respectively. The processes of  $e^+e^- \rightarrow D_{(s)}^*\bar{D}_{(s)}^*$  are depicted in Fig. 3 where the tree-level diagram represents the charmonium transitions and the loop diagram illustrates the  $Y(4260)$  contribution via its molecular component. As mentioned earlier, the tree diagram also contains the contribution from the short-distance core of the  $Y(4260)$ .

The effective Lagrangian for the vector charmonium couplings to the virtual photon is described by the vector meson dominance (VMD) model:

$$\mathcal{L}_{V\gamma} = \frac{em_V^2}{f_V} V_\mu A^\mu, \quad (14)$$

while the strong couplings for  $\psi_i$  ( $i = 1, 2, 3$ ) to the  $D_{(s)}^*\bar{D}_{(s)}^*$  meson pairs are as follows [20, 25]:

$$\begin{aligned} \mathcal{L}_{\psi_S D_{(s)}^* \bar{D}_{(s)}^*} &= ig_{\psi_S D_{(s)}^* \bar{D}_{(s)}^*} \psi_S^k [(\delta^{km} \delta^{ln} - \delta^{kn} \delta^{lm} - \delta^{kl} \delta^{mn})(\partial^m D_{(s)}^{*\dagger l} \bar{D}_{(s)}^{*\dagger n} - D_{(s)}^{*\dagger l} \partial^m \bar{D}_{(s)}^{*\dagger n})] + H.c., \\ \mathcal{L}_{\psi_D D_{(s)}^* \bar{D}_{(s)}^*} &= ig_{\psi_D D_{(s)}^* \bar{D}_{(s)}^*} \psi_D^k [(4\delta^{km} \delta^{ln} - \delta^{kn} \delta^{lm} - \delta^{kl} \delta^{mn})(\partial^m D_{(s)}^{*\dagger l} \bar{D}_{(s)}^{*\dagger n} - D_{(s)}^{*\dagger l} \partial^m \bar{D}_{(s)}^{*\dagger n})] + H.c., \end{aligned} \quad (15)$$

where the coupling constants  $g_{\psi_i D_{(s)}^* \bar{D}_{(s)}^*}$  will be determined by fitting the cross section line shapes. Note that  $\psi_S$  and  $\psi_D$  denote the  $S$  and  $D$  wave  $c\bar{c}$  states of  $J^{PC} = 1^{--}$  of which the couplings to  $D_{(s)}^*\bar{D}_{(s)}^*$  are different, and the above forms are obtained assuming heavy quark spin symmetry.



For the  $e^+e^- \rightarrow D^*\bar{D}^*$ , we consider all of the three conventional charmonium states mentioned above and the  $Y(4260)$ , while for the  $e^+e^- \rightarrow D_s^*\bar{D}_s^*$  we only include  $\psi_2$  ( $\psi(4160)$ ) and  $\psi_3$  ( $\psi(4415)$ ) as the contributing charmonium states since  $\psi_1$  ( $\psi(4040)$ ) is far below the threshold of  $D_s^*\bar{D}_s^*$ . The transition amplitudes for  $e^+e^- \rightarrow D_{(s)}^*\bar{D}_{(s)}^*$  can then be expressed as

$$\begin{aligned}
& \mathcal{M}_{e^+e^- \rightarrow D^*\bar{D}^*} \\
&= \bar{v}(q_2)\gamma^i u(q_1) \left\{ (2\delta^{ij}p_1^k + 2\delta^{ik}p_1^j - 2\delta^{jk}p_1^i) \left[ \frac{-e^2 g_{\psi_1 D^* \bar{D}^*} m_{\psi_1}^2 \exp(-2|p_f^2 - p_{10}^2|/\beta^2 + i\theta_1)}{f_{\psi_1} E_{\text{cm}}^2 (E_{\text{cm}}^2 - m_{\psi_1}^2 + im_{\psi_1} \Gamma_{\psi_1})} \right. \right. \\
&+ \left. \frac{-e^2 g_{\psi_3 D^* \bar{D}^*} m_{\psi_3}^2 \exp(-2|p_f^2 - p_{30}^2|/\beta^2 + i\theta_3)}{f_{\psi_3} E_{\text{cm}}^2 (E_{\text{cm}}^2 - m_{\psi_3}^2 + im_{\psi_3} \Gamma_{\psi_3})} + \frac{-e^2 g_Y^{\text{eff}} m_Y \exp(-2|p_f^2 - p_{Y0}^2|/\beta^2)}{f_Y^{\text{eff}} E_{\text{cm}}^2 \mathcal{D}_Y(E_{\text{cm}})} \right] \\
&+ (2\delta^{ij}p_1^k + 2\delta^{ik}p_1^j - 8\delta^{jk}p_1^i) \frac{-e^2 g_{\psi_2 D^* \bar{D}^*} m_{\psi_2}^2 \exp(-2|p_f^2 - p_{20}^2|/\beta^2 + i\theta_2)}{f_{\psi_2} E_{\text{cm}}^2 (E_{\text{cm}}^2 - m_{\psi_2}^2 + im_{\psi_2} \Gamma_{\psi_2})} \\
&+ \left. \frac{-3e^2 y^{\text{eff}} h' g_\pi m_Y}{2\sqrt{2} f_\pi f_Y^{\text{eff}} E_{\text{cm}}^2 \mathcal{D}_Y(E_{\text{cm}})} \left[ 6I^{ijk}(\alpha, \Lambda_\pi) - C^{ijk}(\alpha, \Lambda_\pi) - C^{ikj}(\alpha, \Lambda_\pi) \right] \right\} \epsilon_{D^*}^{j*} \epsilon_{\bar{D}^*}^{k*}, \quad (16)
\end{aligned}$$

$$\begin{aligned}
& \mathcal{M}_{e^+e^- \rightarrow D_s^*\bar{D}_s^*} \\
&= \bar{v}(q_2)\gamma^i u(q_1) \left\{ (2\delta^{ij}p_1^k + 2\delta^{ik}p_1^j - 8\delta^{jk}p_1^i) \frac{-e^2 g_{\psi_2 D_s^* \bar{D}_s^*} m_{\psi_2}^2 \exp(-2|p_f^2 - p_{20}^2|/\beta^2 + i\theta_4)}{f_{\psi_2} E_{\text{cm}}^2 (E_{\text{cm}}^2 - m_{\psi_2}^2 + im_{\psi_2} \Gamma_{\psi_2})} \right. \\
&+ (2\delta^{ij}p_1^k + 2\delta^{ik}p_1^j - 2\delta^{jk}p_1^i) \left[ \frac{-e^2 g_{\psi_3 D_s^* \bar{D}_s^*} m_{\psi_3}^2 \exp(-2|p_f^2 - p_{30}^2|/\beta^2 + i\theta_5)}{f_{\psi_3} E_{\text{cm}}^2 (E_{\text{cm}}^2 - m_{\psi_3}^2 + im_{\psi_3} \Gamma_{\psi_3})} \right. \\
&+ \left. \left. \frac{-e^2 g_Y^{\text{eff}} m_Y \exp(-2|p_f^2 - p_{Y0}^2|/\beta^2)}{f_Y^{\text{eff}} E_{\text{cm}}^2 \mathcal{D}_Y(E_{\text{cm}})} \right] \right. \\
&+ \left. \frac{-2e^2 y^{\text{eff}} h' g_\pi m_Y}{\sqrt{2} f_\pi f_Y^{\text{eff}} E_{\text{cm}}^2 \mathcal{D}_Y(E_{\text{cm}})} \left[ 6I^{ijk}(\alpha, \Lambda_K) - C^{ijk}(\alpha, \Lambda_K) - C^{ikj}(\alpha, \Lambda_K) \right] \right\} \epsilon_{D_s^*}^{j*} \epsilon_{\bar{D}_s^*}^{k*}, \quad (17)
\end{aligned}$$

where  $q_1$  and  $q_2$  are the incoming four-momenta of the electron and positron, respectively,  $\vec{p}_1$  is the outgoing momentum of  $D_{(s)}^*$  in the c.m. frame,  $p_f = |\vec{p}_1| = \sqrt{E_{\text{cm}}^2 - 4m_{D_{(s)}^*}^2}/2$  is the magnitude of the c.m. momentum of the final state, and  $p_{i0} = \sqrt{m_{\psi_i}^2 - 4m_{D_{(s)}^*}^2}/2$  is the magnitude of the momentum when the c.m. energy is fixed to the intermediate charmonium mass. Note that the pion and kaon propagators are implicated for the exchanged light mesons in the loop functions in Eqs. (16) and (17), respectively. The Gaussian form factor suppresses the resonance contributions when they become far off-shell, and the parameter  $\beta$  controls the suppression. As a reasonable assumption to reduce the number of parameters, we assume that these two processes share the same value for  $\beta$  which means that the strong couplings for  $\psi_i$  to  $D^*\bar{D}^*$  and  $D_s^*\bar{D}_s^*$  have the same suppression behavior when the resonances become off-shell. The  $\psi_i$  states and the  $Y(4260)$  can interfere through many possible intermediate hadron loops which can introduce energy-dependent complex phases. In order to parameterize such effects, we also introduce a few constant phases,

TABLE I. The masses, total widths and leptonic partial widths adopted for the charmonium states from PDG [28].

	$\psi(4040)$	$\psi(4160)$	$\psi(4415)$
$m_\psi$ (MeV)	$4039 \pm 1$	$4191 \pm 5$	$4421 \pm 4$
$\Gamma_\psi$ (MeV)	$80 \pm 10$	$70 \pm 10$	$62 \pm 20$
$\Gamma_{e^+e^-}$ (keV)	$0.86 \pm 0.07$	$0.48 \pm 0.22$	$0.58 \pm 0.07$

denoted by  $\theta_i$ . The constant phase assumption is reasonable as long as the thresholds of the intermediate hadrons are far away. Based on the above argument and taking into account the SU(3) flavor symmetry, we let  $\theta_4 = \theta_2$  and  $\theta_5 = \theta_3$  to reduce two more parameters.

In Eq. (16)  $y^{\text{eff}}/[f_Y^{\text{eff}}\mathcal{D}_Y(E_{\text{cm}})]$  is the product of the bare coupling  $y/f_Y$  and the  $Y(4260)$  propagator defined in the molecular picture [8] which has the following expression:

$$\frac{y^{\text{eff}}}{f_Y^{\text{eff}}\mathcal{D}_Y(E_{\text{cm}})} \equiv \frac{Zy}{2f_Y[E_{\text{cm}} - m_Y - Z\tilde{\Sigma}_1(E_{\text{cm}}) + i\Gamma^{\text{non-}\bar{D}D_1}/2]}, \quad (18)$$

where the subtracted self-energy  $\tilde{\Sigma}_1(E_{\text{cm}}) = \Sigma_1(E_{\text{cm}}) - \text{Re}\Sigma_1(m_Y) - (E - m_Y)\partial\Sigma_1(m_Y)/\partial E_{\text{cm}}$  [26] with  $\Sigma_1(E_{\text{cm}})$  the  $Y(4260)$  self-energy due to the  $\bar{D}D_1(2420)$  loop. In the  $\overline{\text{MS}}$  subtraction scheme, the self-energy is given by  $\Sigma_1(E_{\text{cm}}) = \mu/(8\pi)\sqrt{2\mu(E_{\text{cm}} - m_D - m_{D_1}) + i\mu\Gamma_{D_1}}$  [8]. We use  $m_Y = (4.217 \pm 0.002)$  GeV and  $\Gamma^{\text{non-}\bar{D}D_1} = (0.056 \pm 0.003)$  GeV are determined in the combined analysis of  $e^+e^- \rightarrow J/\psi\pi\pi$  and  $h_c\pi\pi$  [7], and the wave function renormalization constant  $Z \simeq 0.13$  is determined in Ref. [8]. The values of  $m_{\psi_i}$ ,  $\Gamma_{\psi_i \rightarrow e^+e^-}$  and  $\Gamma_{\psi_i}$  ( $i = 1, 2, 3$ ) are taken from those given by the Particle Data Group (PDG) [28], which are listed in Table I. The leptonic decay coupling constants of the charmonium states defined by the VMD model in Eq. (14) can thus be determined.

To further reduce the number of parameters we assume the SU(3) flavor symmetry for the strong couplings of the same charmonium states to  $D^*\bar{D}^*$  and  $D_s^*\bar{D}_s^*$  so that they take the same value, i.e.  $g_{\psi_2 D^*\bar{D}^*} = g_{\psi_2 D_s^*\bar{D}_s^*}$  and  $g_{\psi_3 D^*\bar{D}^*} = g_{\psi_3 D_s^*\bar{D}_s^*}$ . In total there are 11 parameters to be fitted from the cross section data: four cutoff parameters ( $\alpha$ ,  $\Lambda_\pi$ ,  $\Lambda_K$  and  $\beta$ ), four coupling constants ( $g_{\psi_i D^*\bar{D}^*}$  and  $g_{Y D^*\bar{D}^*}^{\text{eff}}$  which is the coupling of the short-distance core of the  $Y(4260)$  to the  $D^*\bar{D}^*$ ), and three phases. We note in advance that due to the lack of precise experimental measurements for the  $e^+e^- \rightarrow D_s^*\bar{D}_s^*$  some of the parameters cannot be well constrained in the numerical fitting, and we anticipate that the main contributions to the  $\chi^2$  value will be from the  $D^*\bar{D}^*$  channel.

In Table II the values of the fitted parameters are listed. The value of  $\beta$ , which bears a large uncertainty, is consistent with the reasonable order of 1 GeV. The cutoff parameter  $\alpha$  is consistent

TABLE II. Parameters determined by fitting to the Belle experimental data [16, 17].

Parameters	Fitted values
$\alpha$	$(1.01 \pm 0.12)$
$\beta$	$(3.58 \pm 2.34)$ GeV
$\Lambda_\pi$	$(409.1 \pm 23.9)$ MeV
$\Lambda_K$	$(544.7 \pm 71.9)$ MeV
$\theta_1$	$132.97^\circ \pm 19.20^\circ$
$\theta_{2,4}$	$229.06^\circ \pm 106.42^\circ$
$\theta_{3,5}$	$284.32^\circ \pm 58.05^\circ$
$g_{\psi_1 D^* \bar{D}^*}$	$(1.96 \pm 0.12)$ GeV $^{-3/2}$
$g_{\psi_2 D_{(s)}^* \bar{D}_{(s)}^*}$	$(0.11 \pm 0.13)$ GeV $^{-3/2}$
$g_{\psi_3 D_{(s)}^* \bar{D}_{(s)}^*}$	$(0.18 \pm 0.06)$ GeV $^{-3/2}$
$g_{Y D_{(s)}^* \bar{D}_{(s)}^*}^{\text{eff}}$	$(0.32 \pm 0.12)$ GeV $^{-3/2}$
$\chi^2/\text{d.o.f}$	1.53

TABLE III. The partial decay widths of  $Y(4260)$  and  $\psi_i$  to  $D_{(s)}^* \bar{D}_{(s)}^*$  extracted from this analysis.

Widths	$Y(4260)$	$\psi(4040)$	$\psi(4160)$	$\psi(4415)$
$\Gamma_{Y D^* \bar{D}^*}^{\text{Tree}}$ (MeV)	$9.50 \pm 7.18$	-	-	-
$\Gamma_{Y D^* \bar{D}^*}^{\text{Loop}}$ (MeV)	$1.27 \pm 0.68$	-	-	-
$\Gamma_{D^* \bar{D}^*}$ (MeV)	$10.77 \pm 7.86$	$10.22 \pm 1.47$	$4.74 \pm 11.73$	$8.52 \pm 5.93$
$\Gamma_{D_s^* \bar{D}_s^*}$ (MeV)	-	-	-	$3.36 \pm 2.34$

with  $\mathcal{O}(1)$ . The cutoff  $\Lambda_\pi$  can be better constrained in  $e^+e^- \rightarrow D^* \bar{D}^*$  than  $\Lambda_K$  in  $e^+e^- \rightarrow D_s^* \bar{D}_s^*$ , again due to the poor data quality of the latter. With the fitted  $\alpha$  and  $\Lambda_\pi$  values, the contribution from the  $\bar{D}D_1(2420)$  intermediate states to the partial decay width for  $Y(4260) \rightarrow D^* \bar{D}^*$  is given by  $\Gamma_{Y(4260) \rightarrow D^* \bar{D}^*}^{\text{Loop}} = (1.27 \pm 0.68)$  MeV, while the contribution from the short-distance  $^3S_1 c\bar{c}$  core is much larger as listed in Table III. With the fitted couplings for the charmonium states to  $D^* \bar{D}^*$  and  $D_s^* \bar{D}_s^*$ , we can also obtain their corresponding partial decay widths which are also listed in Table III.

With the fitted parameters in Table II, we find that the cross section of  $e^+e^- \rightarrow D^* \bar{D}^*$  can be well described. The line shape from the best fit is plotted in Fig. 4 and compared with the Belle data [16]. An apparent feature is that the threshold enhancement in the measured  $e^+e^- \rightarrow D^* \bar{D}^*$  line shape can be largely accounted for by the  $\psi(4040)$  while the contributions from  $Y(4260)$  and

other charmonium states are rather small below 4.2 GeV. The bump between 4.1 and 4.2 GeV can be described well by the contributions from  $\psi(4040)$  and  $\psi(4160)$  and their interference. Notice that the relative phase between these two states leads to destructive interference in the energy regions of below  $\psi(4040)$  or above  $\psi(4160)$  while in the region between their masses the interference is constructive. As a result, the rise of the cross section in the near threshold region is enhanced, although the  $\psi(4040)$  coupling to  $D^*\bar{D}^*$  is in a  $P$  wave.

Comparing the dotted curve (denoted by “ $\psi_i$ ” in the figure), which is the sum of the contributions from all considered conventional charmonium states, with the solid curve, which is the best fit result, or with the experimental data, one sees that the dip around 4.22 GeV in the data comes from a destructive interference between the charmonia and the  $Y(4260)$ . The good description of the special shape around 4.3 GeV originates from the strong coupling of the  $Y(4260)$  to the  $\bar{D}D_1(2420) + c.c.$  (see also the curve denoted by “ $Y$ -loop”), which is an essential feature of the considered hadronic molecular picture. Although the cross section line shape plotted in Fig. 4 is not perfectly fitted, it can still clarify the role played by  $Y(4260)$ . The dominance of the  $\psi(4040)$  and  $\psi(4160)$  near threshold actually leaves a very limited space for the  $Y(4260)$  which is consistent with the expectation based on the hadronic molecule scenario for the  $Y(4260)$ . In other words, the  $Y(4260)$  does not have a large partial decay width in the  $D^*\bar{D}^*$  channel.

We also tried a fit without including the  $Y(4260)$ , and found that the cross section at energies above the dip, which correspond to the region around the  $\bar{D}D_1(2420) + c.c.$  threshold, cannot be well described. In fact, a negligibly small contribution from the  $Y(4260)$  is consistent with the molecular picture.

From Fig. 4 we also see that the cross sections in the region of 4.4  $\sim$  4.6 GeV can be well described by the interference between the  $\psi(4415)$  and the  $Y(4260)$ . Despite this, we need to mention that the  $S$ -wave open thresholds of  $D^*\bar{D}_1(2420) + c.c.$  and  $D^*\bar{D}_2(2460) + c.c.$  have not been taken into account, and they could play a role in the region between 4.4 and 4.5 GeV. We leave their contributions to be investigated more elaborately in future studies when more data are available.

The transition of Fig. 3 (b) has also access to the kinematics of the so-called “triangle singularity” (TS), which has been broadly investigated recently in the literature [29–43] (see e.g. Refs. [5, 44] for a recent review). For an appropriate input energy of the initial  $e^+e^-$  annihilation, the TS condition corresponds to that the internal particles can approach their on-shell kinematics simultaneously and the interactions at all vertices can happen as classical processes in space-time. With all the intermediate mesons fixed as  $D_1\bar{D}\pi$  as in the figure and final states being  $D^{*+}D^{*-}$ ,

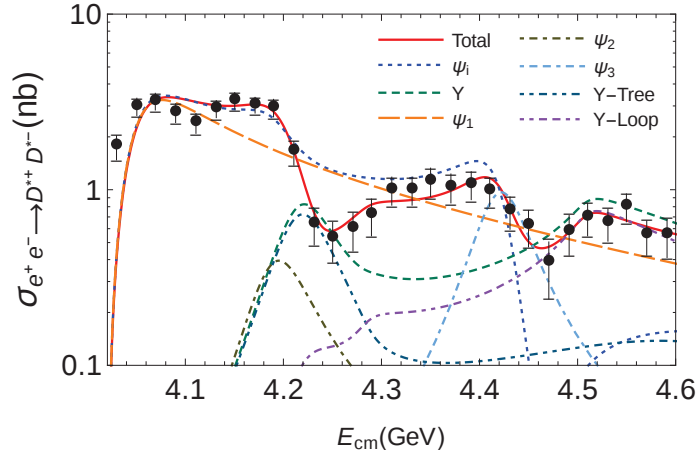


FIG. 4. The fitting results for the cross section of  $e^+e^- \rightarrow D^{*+}D^{*-}$ . The overall cross section is denoted by the solid line. The exclusive contributions from single states are also presented, i.e.  $\psi(4040)$  (long-dashed),  $\psi(4160)$  (dot-dashed),  $\psi(4415)$  (dot-dashed-dashed), and  $Y(4260)$  (dashed). The sum of the contributions from all  $\psi_i$  states is denoted by the dotted line. The data are from Ref. [16].

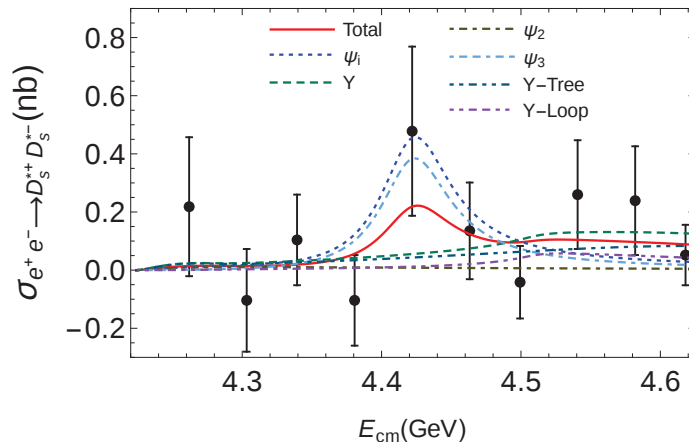


FIG. 5. The fitting results for the cross section of  $e^+e^- \rightarrow D_s^{*+}D_s^{*-}$ . The overall cross section is denoted by the solid line. The exclusive contributions from single states are also presented, i.e.  $\psi(4160)$  (dot-dashed) and  $\psi(4415)$  (dot-dashed-dashed), and  $Y(4260)$  (dashed). The inclusive contributions from  $\psi_i$  is denoted by the dotted line. The data are from Ref. [17].

the  $e^+e^-$  c.m. energy for producing a TS is at about 5.35 GeV which is far beyond the region of Fig. 4. This situation is very different from the cases of  $e^+e^- \rightarrow \bar{D}D^*\pi$  [7, 8] and  $J/\psi\pi\pi$  [19, 45].

As already mentioned the present experimental data for  $e^+e^- \rightarrow D_s^*\bar{D}_s^*$  [17] do not allow a reliable determination of the parameters in this channel. As shown in Fig. 5, with the present fitted parameters only the  $\psi(4415)$  can produce a resonance structure in the cross section line shape. The exclusive contributions from these three states are also presented. The theoretical

curve shows a flattened line shape near threshold which is different from that in  $e^+e^- \rightarrow D^*\bar{D}^*$ . Although the  $D_s^{*+}D_s^{*-}$  threshold, 4.22 GeV, is very close to the mass of the  $Y(4260)$ , we do not see a near-threshold enhancement due to the  $Y(4260)$ . We expect that the contribution of the  $Y(4260)$  in this process should be smaller than that in the  $e^+e^- \rightarrow D^{*+}D^{*-}$  since the intermediate kaon in Fig. 3 (b) cannot go on shell, contrary to the case of the pion. However, one notices that the poor data quality do not allow a more quantitative restriction on the  $Y(4260)$  contribution to this process. This situation is also reflected by the poor determination of the cutoff energy  $\Lambda_K$  shown in Table II. A more precise measurement of the  $e^+e^- \rightarrow D_s^*\bar{D}_s^*$  cross section line shape is highly recommended.

#### IV. SUMMARY

In this work we have studied the cross section line shapes of the  $e^+e^- \rightarrow D^*\bar{D}^*$  and  $D_s^*\bar{D}_s^*$  processes from thresholds to about 4.6 GeV. This is the energy region that contributions from the  $Y(4260)$  are of great interest since information in addition to those in other processes about the structure of this mysterious state can be extracted. Our study shows that the cross sections of these two processes in this energy region are dominated by the established charmonium states, i.e.  $\psi(4040)$ ,  $\psi(4160)$  and  $\psi(4415)$ , while the contributions from the  $Y(4260)$  as a  $D\bar{D}_1(2420) + c.c.$  molecule state turns out to be rather small in most of the energy region. This result is consistent with the observation that the main open charm decay channel of the  $Y(4260)$  is  $D\bar{D}^*\pi + c.c.$  which accounts for most of its decay width. The partial decay width of the  $Y(4260) \rightarrow D^*\bar{D}^*$  is obtained to be  $(11 \pm 8)$  MeV. The dip around 4.22 GeV in the  $e^+e^- \rightarrow D^*\bar{D}^*$  cross section is due to the interference between the  $Y(4260)$  and the conventional charmonium states. The hadronic molecular feature of the  $Y(4260)$  in our model shows up as a non-trivial structure at the  $D\bar{D}_1(2420)$  threshold. The current data present a clear evidence for such a structure. Yet, more precise data are necessary to make the conclusion more solid. For the  $e^+e^- \rightarrow D_s^*\bar{D}_s^*$  channel, the present experimental data from Belle [17] have poor quality. However, although the data do not allow any conclusion on the role played by charmonium states, we do not expect sizeable contributions from the  $Y(4260)$ . The future precise data from BESIII for these two channels will be able to clarify the role played by the  $Y(4260)$  and provide valuable insights into its internal structure.

## ACKNOWLEDGMENTS

Useful discussions with K.-T. Chao and C.-Z. Yuan are acknowledged. We are also grateful to U.-G. Meißner for a careful reading of the manuscript. This work is supported, in part, by the National Natural Science Foundation of China (NSFC) under Grant Nos. 11425525, 11521505 and 11647601, by DFG and NSFC through funds provided to the Sino-German CRC 110 “Symmetries and the Emergence of Structure in QCD” (NSFC Grant No. 11261130311), by the National Key Basic Research Program of China under Contract No. 2015CB856700, by the Thousand Talents Plan for Young Professionals, and by the CAS Key Research Program of Frontier Sciences under Grant No. QYZDB-SSW-SYS013.

- 
- [1] B. Aubert *et al.* [BaBar Collaboration], Phys. Rev. Lett. **95**, 142001 (2005) [hep-ex/0506081].
  - [2] H.-X. Chen, W. Chen, X. Liu and S.-L. Zhu, Phys. Rept. **639**, 1 (2016) [arXiv:1601.02092 [hep-ph]].
  - [3] R. F. Lebed, R. E. Mitchell and E. S. Swanson, Prog. Part. Nucl. Phys. **93**, 143 (2017) [arXiv:1610.04528 [hep-ph]].
  - [4] A. Esposito, A. Pilloni and A. D. Polosa, Phys. Rept. **668**, 1 (2016) [arXiv:1611.07920 [hep-ph]].
  - [5] F.-K. Guo, C. Hanhart, U.-G. Meißner, Q. Wang, Q. Zhao and B. S. Zou, arXiv:1705.00141 [hep-ph].
  - [6] Q. Wang, M. Cleven, F.-K. Guo, C. Hanhart, U.-G. Meißner, X.-G. Wu and Q. Zhao, Phys. Rev. D **89**, 034001 (2014) [arXiv:1309.4303 [hep-ph]].
  - [7] M. Cleven, Q. Wang, F.-K. Guo, C. Hanhart, U.-G. Meißner and Q. Zhao, Phys. Rev. D **90**, 074039 (2014) [arXiv:1310.2190 [hep-ph]].
  - [8] W. Qin, S.-R. Xue and Q. Zhao, Phys. Rev. D **94**, 054035 (2016) [arXiv:1605.02407 [hep-ph]].
  - [9] M. Ablikim *et al.* [BESIII Collaboration], Phys. Rev. Lett. **110**, 252001 (2013) [arXiv:1303.5949 [hep-ex]].
  - [10] M. Ablikim *et al.* [BESIII Collaboration], Phys. Rev. Lett. **111**, 242001 (2013) [arXiv:1309.1896 [hep-ex]].
  - [11] M. Ablikim *et al.* [BESIII Collaboration], Phys. Rev. Lett. **112**, 022001 (2014) [arXiv:1310.1163 [hep-ex]].
  - [12] M. Ablikim *et al.* [BESIII Collaboration], Phys. Rev. Lett. **113**, 212002 (2014) [arXiv:1409.6577 [hep-ex]].
  - [13] M. Ablikim *et al.* [BESIII Collaboration], Phys. Rev. Lett. **115**, 112003 (2015) [arXiv:1506.06018 [hep-ex]].
  - [14] M. Ablikim *et al.* [BESIII Collaboration], Phys. Rev. Lett. **115**, 182002 (2015) [arXiv:1507.02404 [hep-ex]].

- [15] X. Y. Gao, C. P. Shen and C. Z. Yuan, Phys. Rev. D **95**, no. 9, 092007 (2017) doi:10.1103/PhysRevD.95.092007 [arXiv:1703.10351 [hep-ex]].
- [16] K. Abe *et al.* [Belle Collaboration], Phys. Rev. Lett. **98**, 092001 (2007) [hep-ex/0608018].
- [17] G. Pakhlova *et al.* [Belle Collaboration], Phys. Rev. D **83**, 011101 (2011) [arXiv:1011.4397 [hep-ex]].
- [18] M.-L. Du, U.-G. Meißner and Q. Wang, Phys. Rev. D **94**, 096006 (2016) [arXiv:1608.02537 [hep-ph]].
- [19] Q. Wang, C. Hanhart and Q. Zhao, Phys. Rev. Lett. **111**, 132003 (2013) [arXiv:1303.6355 [hep-ph]].
- [20] F.-K. Guo, C. Hanhart, U.-G. Meißner, Q. Wang and Q. Zhao, Phys. Lett. B **725**, 127 (2013) [arXiv:1306.3096 [hep-ph]].
- [21] M. Cleven and Q. Zhao, Phys. Lett. B **768**, 52 (2017) [arXiv:1611.04408 [hep-ph]].
- [22] F.-K. Guo, C. Hanhart and U.-G. Meißner, Phys. Rev. Lett. **103**, 082003 (2009) Erratum: [Phys. Rev. Lett. **104**, 109901 (2010)] [arXiv:0907.0521 [hep-ph]].
- [23] F.-K. Guo, C. Hanhart, G. Li, U.-G. Meißner and Q. Zhao, Phys. Rev. D **83**, 034013 (2011) [arXiv:1008.3632 [hep-ph]].
- [24] X. Li and M. B. Voloshin, Phys. Rev. D **88**, 034012 (2013) [arXiv:1307.1072 [hep-ph]].
- [25] A. Margaryan and R. P. Springer, Phys. Rev. D **88**, 014017 (2013) [arXiv:1304.8101 [hep-ph]].
- [26] M. Cleven, F.-K. Guo, C. Hanhart and U.-G. Meißner, Eur. Phys. J. A **47**, 120 (2011) [arXiv:1107.0254 [hep-ph]].
- [27] Z. Cao, M. Cleven, Q. Wang and Q. Zhao, Eur. Phys. J. C **76**, 601 (2016) [arXiv:1608.07947 [hep-ph]].
- [28] C. Patrignani *et al.* [Particle Data Group], Chin. Phys. C **40**, 100001 (2016).
- [29] J.-J. Wu, X.-H. Liu, Q. Zhao and B.-S. Zou, Phys. Rev. Lett. **108**, 081803 (2012) [arXiv:1108.3772 [hep-ph]].
- [30] X.-G. Wu, J.-J. Wu, Q. Zhao and B.-S. Zou, Phys. Rev. D **87**, 014023 (2013) [arXiv:1211.2148 [hep-ph]].
- [31] X.-H. Liu and G. Li, Phys. Rev. D **88**, 014013 (2013) [arXiv:1306.1384 [hep-ph]].
- [32] X. H. Liu, Phys. Rev. D **90**, 074004 (2014) [arXiv:1403.2818 [hep-ph]].
- [33] A. P. Szczepaniak, Phys. Lett. B **747**, 410 (2015) [arXiv:1501.01691 [hep-ph]].
- [34] X.-H. Liu, M. Oka and Q. Zhao, Phys. Lett. B **753**, 297 (2016) [arXiv:1507.01674 [hep-ph]].
- [35] F.-K. Guo, U.-G. Meißner, W. Wang and Z. Yang, Phys. Rev. D **92**, 071502 (2015) [arXiv:1507.04950 [hep-ph]].
- [36] X.-H. Liu, Q. Wang and Q. Zhao, Phys. Lett. B **757**, 231 (2016) [arXiv:1507.05359 [hep-ph]].
- [37] A. P. Szczepaniak, Phys. Lett. B **757**, 61 (2016) [arXiv:1510.01789 [hep-ph]].
- [38] F.-K. Guo, U.-G. Meißner, J. Nieves and Z. Yang, Eur. Phys. J. A **52**, 318 (2016) [arXiv:1605.05113 [hep-ph]].
- [39] M. Bayar, F. Aceti, F.-K. Guo and E. Oset, Phys. Rev. D **94**, 074039 (2016) [arXiv:1609.04133 [hep-ph]].
- [40] Z. Yang, Q. Wang and U.-G. Meißner, Phys. Lett. B **767**, 470 (2017) [arXiv:1609.08807 [hep-ph]].
- [41] E. Wang, J. J. Xie, W. H. Liang, F.-K. Guo and E. Oset, Phys. Rev. C **95**, 015205 (2017) [arXiv:1610.07117 [hep-ph]].
- [42] A. Pilloni *et al.* [JPAC Collaboration], Phys. Lett. B **772**, 200 (2017) [arXiv:1612.06490 [hep-ph]].



- [43] Q. R. Gong, J. L. Pang, Y. F. Wang and H. Q. Zheng, arXiv:1612.08159 [hep-ph].
- [44] Q. Zhao, JPS Conf. Proc. **13**, 010008 (2017).
- [45] Q. Wang, C. Hanhart and Q. Zhao, Phys. Lett. B **725**, 106 (2013) [arXiv:1305.1997 [hep-ph]].